Schizophrenia Bulletin vol. 49 no. 1 pp. 196–207, 2023
https://doi.org/10.1093/schbul/sbac113
Advance Access publication September 6, 2022

Multimodal Magnetic Resonance Imaging Depicts Widespread and Subregion Specific Anomalies in the Thalamus of Early-Psychosis and Chronic Schizophrenia Patients

Yasser Alemán-Gómez[1,2,*], Thomas Baumgartner[3], Paul Klauser[2,4], Martine Cleusix[2], Raoul Jenni[2], Patric Hagmann[1], Philippe Conus[5], Kim Q. Do[2], Meritxell Bach Cuadra[6,1], Philipp S. Baumann[5], and Pascal Steullet[2]

[1]Department of Radiology, Centre Hospitalier Universitaire Vaudois (CHUV) and University of Lausanne (UNIL), Lausanne, Switzerland; [2]Department of Psychiatry, Center for Psychiatric Neuroscience, Centre Hospitalier Universitaire Vaudois (CHUV) and University of Lausanne (UNIL), Prilly, Switzerland; [3]Department of Clinical Neurosciences, Centre Hospitalier Universitaire Vaudois (CHUV) and University of Lausanne (UNIL), Lausanne, Switzerland; [4]Department of Psychiatry, Service of Child and Adolescent Psychiatry, Centre Hospitalier Universitaire Vaudois (CHUV) and University of Lausanne (UNIL), Lausanne, Switzerland; [5]Department of Psychiatry, Service of General Psychiatry, Centre Hospitalier Universitaire Vaudois (CHUV) and University of Lausanne (UNIL), Lausanne, Switzerland; [6]Medical Image Analysis Laboratory (MIAL), Centre d'Imagerie BioMédicale (CIBM), Switzerland

*To whom correspondence should be addressed; Centre de Recherche en Radiologie. Rue Centrale 7, CH-1003 Lausanne. Switzerland; tel: +41213241537, e-mail: yasseraleman@gmail.com

***Background and Hypothesis*: Although the thalamus has a central role in schizophrenia pathophysiology, contributing to sensory, cognitive, and sleep alterations, the nature and dynamics of the alterations occurring within this structure remain largely elusive. Using a multimodal magnetic resonance imaging (MRI) approach, we examined whether anomalies: (1) differ across thalamic subregions/nuclei, (2) are already present in the early phase of psychosis (EP), and (3) worsen in chronic schizophrenia (SCHZ). *Study Design*: T1-weighted and diffusion-weighted images were analyzed to estimate gray matter concentration (GMC) and microstructural parameters obtained from the spherical mean technique (intra-neurite volume fraction [VF_{INTRA})], intra-neurite diffusivity [$DIFF_{INTRA}$], extra-neurite mean diffusivity [MD_{EXTRA}], extra-neurite transversal diffusivity [TD_{EXTRA}]) within 7 thalamic subregions. *Results*: Compared to age-matched controls, the thalamus of EP patients displays previously unreported widespread microstructural alterations (VF_{INTRA} decrease, TD_{EXTRA} increase) that are associated with similar alterations in the whole brain white matter, suggesting altered integrity of white matter fiber tracts in the thalamus. In both patient groups, we also observed more localized and heterogenous changes (either GMC decrease, MD_{EXTRA} increase, or $DIFF_{INTRA}$ decrease) in mediodorsal, posterior, and ventral anterior parts of the thalamus in both patient groups, suggesting that the nature of the alterations varies across subregions. GMC and $DIFF_{INTRA}$ in the whole thalamus correlate with global functioning, while $DIFF_{INTRA}$ in the subregion encompassing the medial pulvinar is significantly associated with negative symptoms in SCHZ. *Conclusion*: Our data reveals both widespread and more localized thalamic anomalies that are already present in the early phase of psychosis.**

Key words: MRI/thalamus/nuclei/microstructure/early-psychosis/schizophrenia

Introduction

The thalamus is a subcortical structure that relays sensory information to the cortex, but also orchestrates various synchronized cortical activities involved in cognitive processes and sleep. Composed of nuclei with distinct connectivities, the thalamus is embedded within multiple brain networks. It constitutes an essential interface between sensory and motor systems, and plays a key role in cognitive and emotional processes. An extensive literature supports that thalamus-related anomalies contribute to the pathology of schizophrenia.[1–5] Reduced thalamic volume, abnormal structural and functional connectivity with the cortex, striatum and cerebellum, and aberrant activation across high-order cognitive domains are reported in schizophrenia patients, but also in high-risk individuals.[6–17] Both postmortem studies and magnetic resonance imaging (MRI) studies report abnormalities mostly in high-order thalamic nuclei.[11,18–29] However, our knowledge about thalamic anomalies in different stages

© The Author(s) 2022. Published by Oxford University Press on behalf of the Maryland Psychiatric Research Center. All rights reserved. For permissions, please email: journals.permissions@oup.com

Downloaded from https://academic.oup.com/schizophreniabulletin/article/49/1/196/6692485 by EPF Lausanne (Inactive) user on 29 March 2023

of the illness remains fragmented. Previous studies have typically investigated the thalamus using a single MRI modality in either high-risk, early psychosis, or chronic schizophrenia.[11,20,21,30] Moreover, only a few studies have assessed the thalamus integrity at the subregion/nucleus level. Therefore, we sought to characterize the microstructural organization of the thalamus at the subregion level by using multimodal MRI data from psychotic patients at different stages (early-psychosis [EP], chronic schizophrenia [SCHZ]) to reveal novel features of the thalamic anomalies and their dynamic changes along the course of the disorder. We hypothesized that, unlike the loss of gray matter (GM) which is localized in some subregions, alterations of diffusion properties, revealing changes in the microstructure, would be more widespread, and occur early during the time course of the disease. Microstructural features were described using 4 diffusion MRI-derived metrics obtained from the spherical mean technique (SMT)[31] and GM concentration (GMC) estimated from T1-weighted imaging. SMT is a two-compartment model for diffusion imaging to estimate microscopic characteristics separately within an intraneurite compartment (composed of fine processes like dendrites and axons) and an extraneurite compartment (composed of cell bodies, extracellular space), irrespective of fiber crossings and orientation dispersion. The intraneurite compartment is described by the intra-neurite volume fraction (VF_{INTRA}) and intra-neurite diffusivity ($DIFF_{INTRA}$); the extraneurite compartment is depicted by the extra-neurite mean diffusivity (MD_{EXTRA}) and extra-neurite transversal diffusivity (TD_{EXTRA}). The SMT model has been validated in animal models[31] and was selected over another widely used approach, NODDI (Neurite orientation dispersion and density imaging)[32] for 2 reasons: (1) NODDI includes a compartment where the diffusion is considered isotropic and this assumption is not applicable to the thalamic anatomy; (2) NODDI arbitrarily sets the diffusivity values while SMT estimates them directly from the data.

GMC was assessed using a partial-volume technique[33] highly sensitive to detect GM decrease in the thalamus of psychotic patients.[27] Because of nonlinear effects of age (between 15 and 60 years old) on some of these MRI parameters,[27] we compared each patient group with age-matched healthy subjects. We examined whether all diffusion- and GM-related anomalies are only restricted to specific subregions and similar within the affected subregions. Most importantly, we looked for abnormalities present during the early stages of the disease that could represent biomarkers. We further investigated whether alterations in GMC and diffusion-derived metrics are closely related and how their relationships are changed in EP and SCHZ compared to their respective control subjects. Moreover, we explored the relationship between diffusion-derived metrics within the thalamus and WM tracts because altered diffusion properties within the thalamus could reflect the altered integrity of fibers entering/exiting the thalamus. Finally, we looked for associations of MRI metrics with symptom's severity and global functioning.

Methods

Participants

Chronic patients meeting DSM-IV criteria for schizophrenia or schizoaffective disorder were recruited from Lausanne University Hospital. Subjects in the early phase of psychosis (within 5 years of a first psychotic episode[34]) were recruited from the Treatment and Early Intervention in Psychosis Program (Lausanne University Hospital).[35] Most patients were taking antipsychotic medication at the time of the study. The average medication was estimated in chlorpromazine equivalent dose (*CPZ*).[36] Forty-two SCHZ and 97 EP, who completed a full MRI scanning session and fulfilled the inclusion criteria were included.

In addition, 139 healthy controls (HCs), recruited from similar geographic and sociodemographic areas, and assessed by the Diagnostic Interview for Genetic Studies (DIGS),[37] were selected and automatically divided into 2 groups (42 HC_{SCHZ} and 97 HC_{EP}) in order to match with each of the patient groups (SCHZ and EP) for gender, age, and handedness (Supplementary Material, Supp.1). Participants provided written informed consents. The study was conducted in accordance with the Declaration of Helsinki and approved by the local Ethics Committee. Major mood, psychotic, or substance-use disorder, and having a first-degree relative with a psychotic disorder were exclusion criteria for HCs. Neurological disorders, severe head trauma, or mental retardation (IQ < 70) were exclusion criteria for all subjects. A subset of participants (23 SCHZ, 41 EP, and 69 HC) were included in a previous study on GM quantification within the thalamus.[27]

Clinical Assessments

Clinical symptoms were evaluated by a trained psychologist using the Positive And Negative Syndrome Scale (PANSS).[38] Functional level was determined using the Global Assessment of Functioning (GAF) scale.[39] Duration of illness was defined as the time between the onset of psychotic symptoms (assessed with the Comprehensive Assessment of At-Risk Mental States, CAARMS[40]) and MRI scanning.

MRI Acquisition

MRI sessions were performed during the same time period as the clinical assessments on 2 different 3-Tesla scanners (Magnetom TrioTim and PRISMA, Siemens Medical Solutions) equipped with a 32-channel head coil each. Each scanning session included a magnetization

Downloaded from https://academic.oup.com/schizophreniabulletin/article/49/1/196/6692485 by EPF Lausanne (Inactive) user on 29 March 2023

prepared rapid acquisition gradient echo (MPRAGE) T1-weighted (T1w) sequence and a spin-echo echo-planar imaging (SE-EPI) diffusion spectrum imaging (DSI) sequence (for more details see Supp.1). Images were visually inspected to guarantee high quality of the dataset. This visual quality control includes exclusion criteria that take into account incidental findings and poor-quality images. Additionally, different quality metrics were computed from T1w[41] and diffusion-weighted images (DWIs)[42] to test if between-group differences in data quality could bias the results (Supp.1 and Supp.2).

Image Processing

Microstructure Maps Estimation

For each subject, an automatic quality-control and image correction workflow was implemented to its DWI data. The workflow employed Mrtrix3[43] and FSL[44] processing suites for performing the following steps: Denoising, bias correction, intensity normalization, head motion correction, eddy current, and distortion correction using Advanced Normalization Tools (ANTs).[45] The corrected dataset was used to obtain different scalar maps with the SMT.[31] SMT models the diffusion signal measured inside the voxel as a linear combination of the diffusion signals coming from 2 different and independent tissue compartments (intra- and extra-neurite compartments). Throughout this approach, the intra-neurite volume fraction (VF_{INTRA}), intra-neurite diffusivity ($DIFF_{INTRA}$), extra-neurite mean diffusivity (MD_{EXTRA}), and extra-neurite transversal diffusivity (TD_{EXTRA}) maps were computed (figure S3).

Gray Matter Concentration Estimation

The T1w image was used to estimate GMC using NISEG, a partial-volume-based tissue segmentation algorithm.[33] This method models the voxel intensity through the mixel model[46] by adding the cerebrospinal fluid (CSF), GM (figure S3E) and white matter (WM) global characteristic intensities weighted by their respective local concentrations with a Gaussian noise with constant standard deviation across tissues.

Thalamic Parcellation

FreeSurfer (v6.0.1) was used to segment the thalamus[47] that was further subdivided, using an atlas-based parcellation approach (figure S3),[27] in 7 subregions (pulvinar [Pul], ventral anterior [VA], mediodorsal [MD], lateral posterior-ventral posterior group [LP-VP], medial pulvinar-centrolateral group [PuM-CL], ventrolateral [VL], ventral posterior-ventrolateral group [VP-VL]). Mean GMC and each SMT-derived metric were obtained for every thalamic subregion.

Statistical Harmonization

A statistical harmonization procedure (ComBat[48]) was applied over the computed measures to reduce the interscanner bias while preserving the intersubject biological variability (figures S4-S6). Age, gender, and disease status were added as covariates to the design matrix.

Statistics

Statistical analyses were performed with the Statistics and Machine Learning Toolbox in Matlab (v.R2020a). Normality of the distributions was checked with a Shapiro test.

Nonparametric Spearman ranks partial correlations were used to test the association with age (figure S7, table ST3) and chlorpromazine equivalents (figure S8, table ST4) and to identify confounders that should be included in the statistical model. To test for group differences in demographics and clinical variables (HC_{EP} vs EP and HC_{SCHZ} vs SCHZ), Student's *t*-tests were used for continuous variables and χ^2 tests for discrete categorical variables.

The mean SMT-based metrics for each region of interest (whole thalamus and subregions) were corrected for age, gender, and its mean value in the WM using multiple regression analyses. The intracranial volume (ICV) was used as covariate for GMC. Unstandardized residuals were used in the main analyses. Thereafter, 4 inferential analyses were conducted.

First, Analyses of Variance (ANOVA) were performed to identify differences between groups for SMT-derived parameters and GMC within the whole thalamus and each subregion of both hemispheres. Post hoc tests (Mann–Whitney U or Student's *t*-test depending on data normality) were then conducted to assess group differences between EP and HC_{EP}, SCHZ and HC_{SCHZ}, and EP with respect to SCHZ.

Second, Pearson correlation coefficients were computed between diffusion-derived metrics quantified inside the thalamus and within the global WM.

Third, Pearson partial correlation was performed to explore direct associations among GMC, VF_{INTRA}, and TD_{EXTRA} inside each region of interest. In this case, values were averaged across both hemispheres. These provided the correlation between each pair of variables while accounting for the effects of all remaining variables.

Finally, the MRI metrics with significant group differences were tested for correlation with the duration of illness, PANSS scores, and GAF in both EP and SCHZ using Pearson's or Spearman's correlation analysis depending on data normality.

Downloaded from https://academic.oup.com/schizophreniabulletin/article/49/1/196/6692485 by EPF Lausanne (Inactive) user on 29 March 2023

A $P < .05$ (two-tailed) was considered significant after controlling for multiple comparisons using the False Discovery Rate (FDR) with $q = 0.05$ [64 comparisons for diffusion-based metrics (8 regions × 2 hemispheres × 4 metrics); 16 (8 regions × 2 hemispheres) for GMC] were performed. For the partial correlation analysis, 24 comparisons (for each group: 8 regions × 3 correlations) were carried out.

Results

Demographics and Clinical Assessment

Table 1 presents the demographic characteristics of the patient cohorts and their respective HCs (HC_{EP} and HC_{SCHZ}). No significant differences between patients and HCs were found for age, gender, or handedness. EP and SCHZ showed significantly lower GAF scores than their respective HCs.

Alterations of Diffusion-derived Parameters and GMC

We first compared microstructural features (VF_{INTRA}, $DIFF_{INTRA}$, MD_{EXTRA}, and TD_{EXTRA}) and GMC within the thalamus of EP and SCHZ, with their respective HCs. We found a significant bilateral decrease of VF_{INTRA} within the whole thalamus and each subregion in EP but not SCHZ (figure 1, table ST7).

A significant $DIFF_{INTRA}$ decrease was limited to the left PuM-CL of EP, with no alterations in SCHZ (figure S9, table ST8). For MD_{EXTRA}, we observed a trend for a bilateral increase in the whole thalamus of EP but not SCHZ (figure S10, table ST9). In EP, bilateral VA and right LP-VP displayed a significant MD_{EXTRA} increase, while the other subregions (except VL and PuM-CL) showed a trend for MD_{EXTRA} increase. In SCHZ, only the right VA showed higher MD_{EXTRA} as compared to HC_{SCHZ}. Regarding TD_{EXTRA}, we observed a bilateral increase within the whole thalamus of EP (figure 1, table ST10). TD_{EXTRA} was significantly higher bilaterally in VA, MD, LP-VP, and VP-VL, and right pulvinar of EP as compared to HC_{EP}. In SCHZ, we found however no TD_{EXTRA} alterations. Noteworthy, SCHZ and EP showed similar values for every diffusion-derived metrics (tables ST12-ST13), indicating that the absence of differences between some of these diffusion-related parameters in SCHZ as compared to HC_{SCHZ} is not due to a recovery of the microstructural organization during the chronic stage.

A significant GMC decrease was found bilaterally in MD, right pulvinar and LP-VP of EP (figure 2, table ST11), and bilaterally in PuM-CL, right MD and LP-VP of SCHZ. However, as compared to EP, SCHZ displayed a trend for lower GMC (table ST14).

Table 1. Demographic and Clinical Variables of Early Psychosis (EP) and Chronic Schizophrenia (SCHZ) Patients, and Their Respective Healthy Controls (HC_{EP}, HC_{SCHZ})

	HC_{EP} ($N = 97$)	EP ($N = 97$)	Statistics U[a], T, χ^2 (P-value)	HC_{SCHZ} ($N = 42$)	SCHZ ($N = 42$)	Statistics U, T, χ^2 (P-value)
Age mean (SD) [range]	24.9 (4.7) [16.2–38.2]	24.7 (5.0) [15.6–38.7]	$U = 0.4$ ($P = .7$)	36.7 (8.2) [24.5–59.1]	38.6 (8.9) [24.7–58.6]	$U = -0.9$ ($P = .3$)
Laterality (right/left/others)	82/13/2	85/9/3	$\chi^2 = 1.1$ ($P = .6$)	33/6/3	36/5/1	$\chi^2 = 1.2$ ($P = .5$)
Duration of illness[b] (days)		634.4 (808.1)			5072.2 (2452.4)	
GAF[c]	83.8 (4.4)	56.2 (11.9)	$U = 11.4$ ($P < 10^{-4}$)	83.7 (4.1)	54.3 (11.8)	$U = 7.0$ ($P < 10^{-4}$)
CPZ[d] equivalent		346.0 (272.6)			346.2 (296.4)	
Typical		2			3	
Atypical		75			33	
Both		3			2	
No medication/ information		17			4	
Symptoms						
PANSSPOS[e]		12.9 (4.2)			14.6 (4.5)	
PANSSNEG		16.1 (5.9)			16.6 (5.5)	
PANSSGEN		32.9 (8.7)			32.7 (8.4)	
PANSSTOTAL		62.0 (15.9)			63.5 (14.6)	

Note:
[a]Comparisons between groups were conducted using the nonparametric Mann–Whitney U test or the parametric Student's t-test. The applied test was based on the normality of data as evaluated by a Shapiro–Wilk test.
[b]Duration of illness was defined as the time between date of onset of first positive symptoms and date of scan acquisition.
[c]GAF, Global Assessment of Functioning scale.
[d]CPZ, antipsychotic medication intake in chlorpromazine equivalents at time of scanning (in mg).
[e]PANSS, Positive and Negative Syndrome Scale.

Downloaded from https://academic.oup.com/schizophreniabulletin/article/49/1/196/6692485 by EPF Lausanne (Inactive) user on 29 March 2023

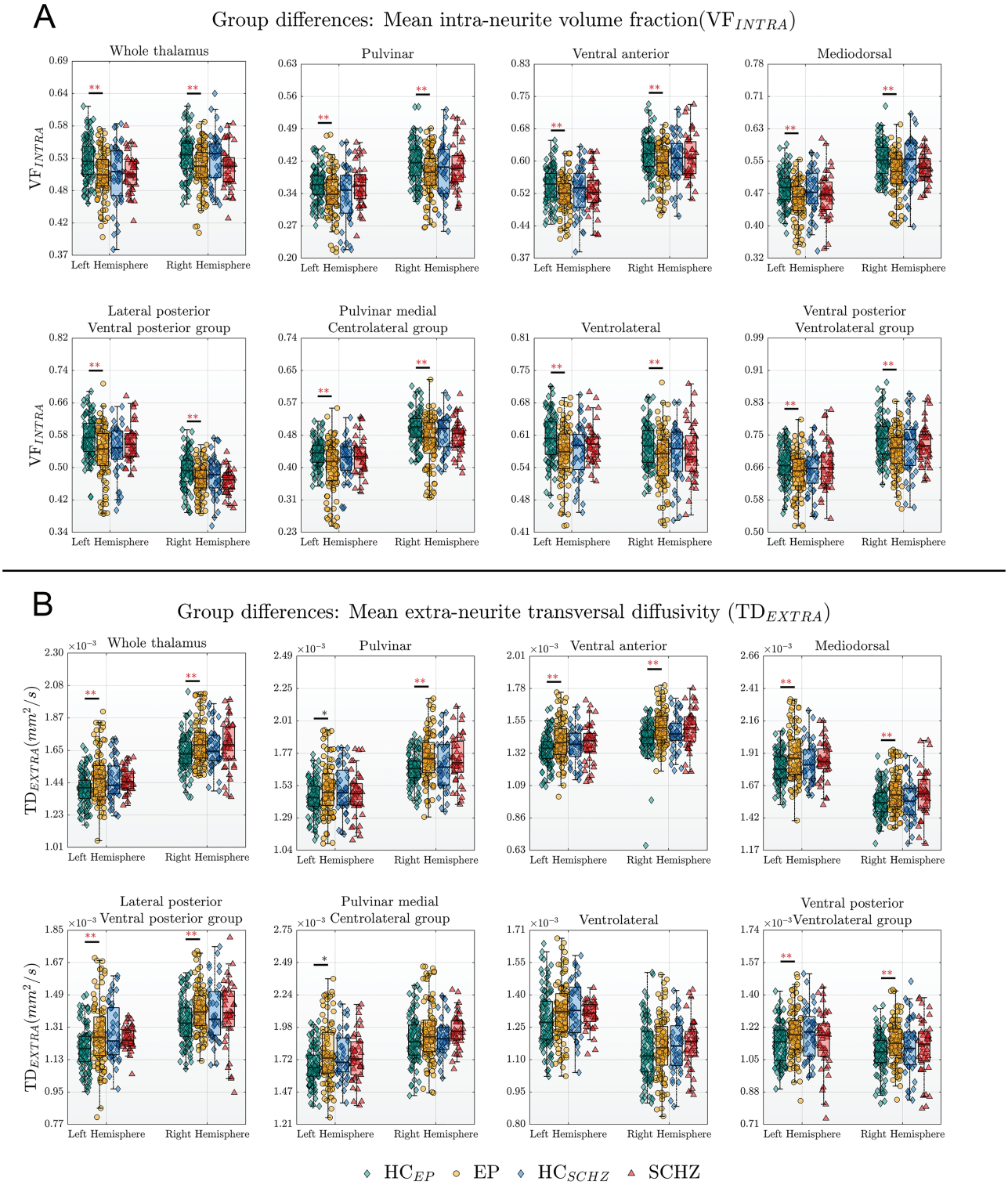

Fig. 1. (A) Intra-neurite volume fraction (VF_{INTRA}) and (B) extra-neurite transversal diffusivity (TD_{EXTRA}) in whole thalamus and its subregions of early-psychosis (EP) (n = 97), SCHZ (n = 42), and their respective controls (HC_{EP}, n = 97; HC_{SCHZ}, n = 42). One or two asterisks indicate differences before ($P < .05$ two-tailed) and after False Discovery Rate (FDR) correction ($q = 0.05$) respectively.

In summary, VF_{INTRA} was homogeneously lower across all thalamic subregions of EP as compared to HC_{EP}. This was accompanied with a widespread increase in TD_{EXTRA} within most subregions. Moreover, EP displayed other types of alterations localized in anterior, mediodorsal, and posterior parts (MD_{EXTRA} increase in VA and LP-VP, $DIFF_{INTRA}$ decrease in PuM-CL, GMC decrease in pulvinar, MD and LP-VP). When compared to HC_{SCHZ},

Downloaded from https://academic.oup.com/schizophreniabulletin/article/49/1/196/6692485 by EPF Lausanne (Inactive) user on 29 March 2023

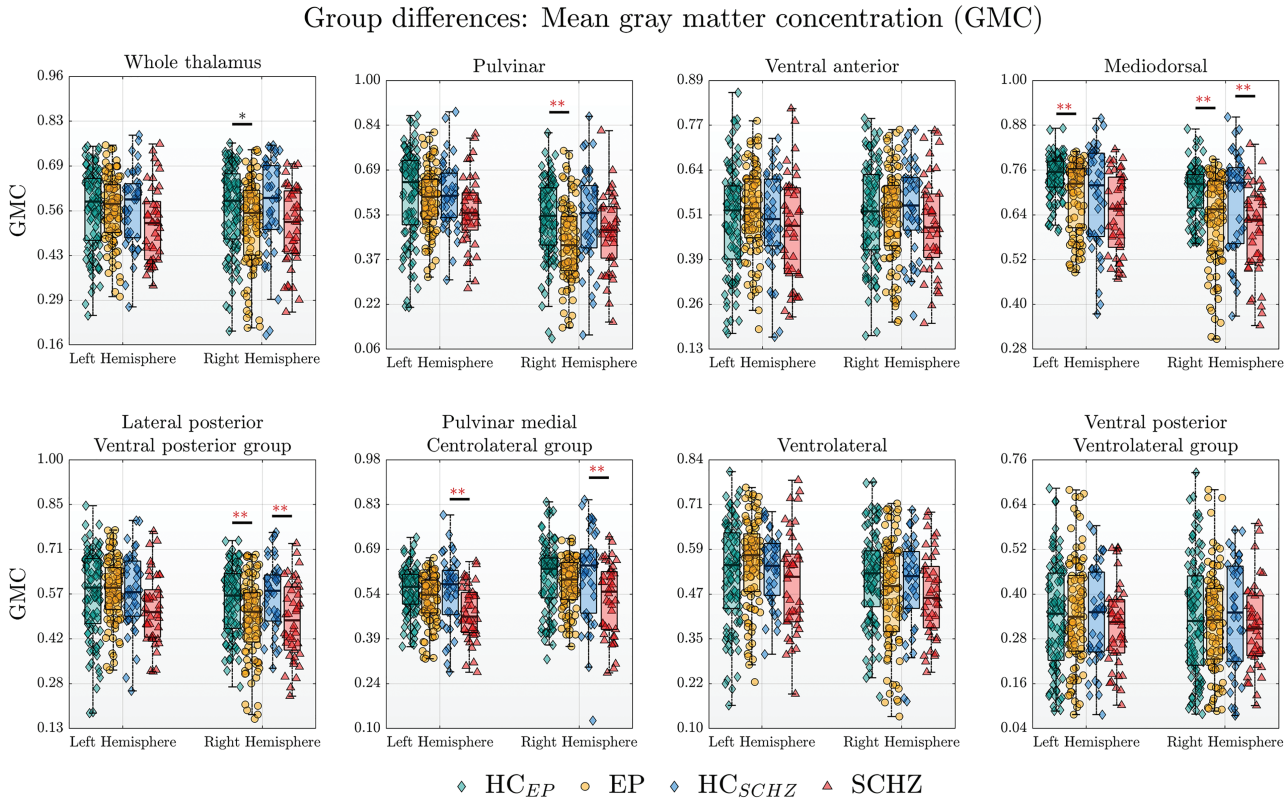

Fig. 2. Gray matter concentration (GMC) in whole thalamus and its subregions of early-psychosis (EP) (n = 97), SCHZ (n = 42), and their respective controls (HC$_{EP}$, n = 97; HC$_{SCHZ}$, n = 42). One or two asterisks indicate differences before (P < .05 two-tailed) and after False Discovery Rate (FDR) correction (q = 0.05) respectively.

SCHZ also showed anomalies in anterior, mediodorsal, and posterior parts (MD$_{EXTRA}$ increased in VA, GMC decrease in PuM-CL, MD, and LP-VP). The lack of VF$_{INTRA}$ and TD$_{EXTRA}$ anomalies in SCHZ as compared to HC$_{SCHZ}$ does not however indicate a normalization of the underlying microstructural anomalies.

Relationships Between Diffusion-derived Parameters in Thalamus and WM

For all subject groups, we observed strong correlations between diffusion-derived parameters (VF$_{INTRA}$, MD$_{EXTRA}$, and TD$_{EXTRA}$, but not DIFF$_{INTRA}$) within the thalamus and the whole WM mask (figure S11, table ST15). In both thalamus and global WM, we detected a decrease of VF$_{INTRA}$, increase in TD$_{EXTRA}$ (figures 1, S11) and MD$_{EXTRA}$ (trend for the whole thalamus, figures S10, S11) in EP, but not SCHZ (table ST16). Thus, these metrics seem to depict alterations of microstructural features common to both thalamus and WM tracts. Despite the use of SMT-based mean values of the whole WM as covariates, VF$_{INTRA}$ decrease and TD$_{EXTRA}$ increase remained significant and widespread across the thalamus of EP. These suggest that VF$_{INTRA}$ and TD$_{EXTRA}$ alterations within the thalamus of EP reflect structural anomalies associated with the fiber tracts entering and/or projecting out of the thalamus. By contrast, the decrease of DIFF$_{INTRA}$ in PuM-CL of EP could indicate local alterations at the level of neurites that are unrelated to WM abnormalities.

Relationships Between Diffusion-derived Parameters and GMC

We further explored the relationships between SMT-derived parameters (which capture the microstructure) and GMC (which provides an estimate of the relative proportion of thalamic GM). As expected, subregions (pulvinar, PuM-CL, MD) with the highest GMC had the lowest VF$_{INTRA}$, while those with the lowest GMC (VP-VL, VA) displayed the highest VF$_{INTRA}$ (figures 1 and 2). However, the widespread VF$_{INTRA}$ decrease within the thalamus of EP, as compared to HC$_{EP}$, was accompanied by a GMC decrease (and not increase) in several mediodorsal and posterior subregions. This suggests that relationships between diffusion-derived parameters and GMC are loose and may change with the nature of the tissue alterations. Therefore, we examined more finely the relationships between VF$_{INTRA}$, TD$_{EXTRA}$, and GMC within subregions by calculating the partial correlations between each of the above MRI parameters. In all groups, we observed significant partial negative

Downloaded from https://academic.oup.com/schizophreniabulletin/article/49/1/196/6692485 by EPF Lausanne (Inactive) user on 29 March 2023

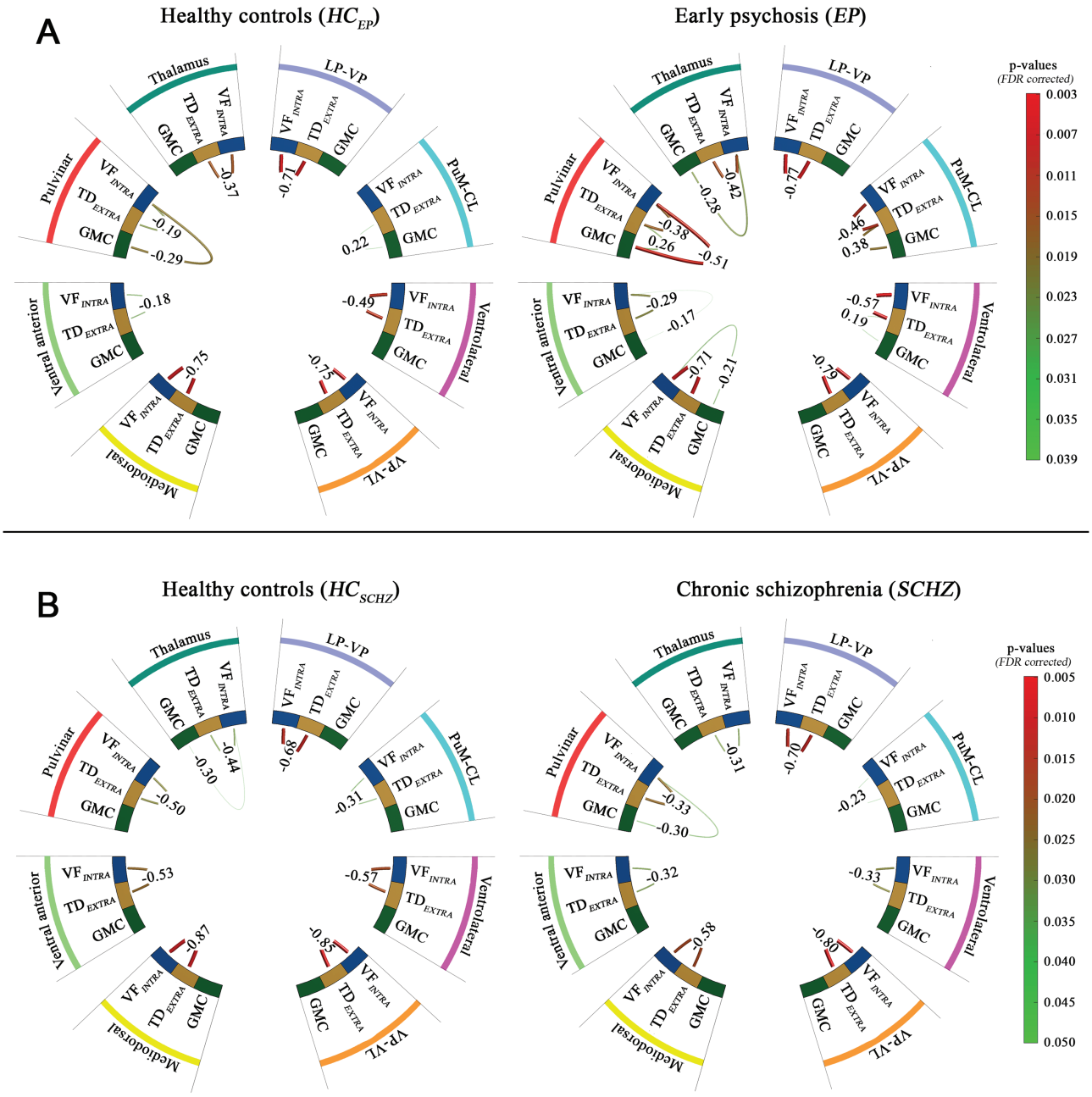

Note: *Numerical values between metrics represent their corresponding partial correlation coefficients.*

Fig. 3. Significant partial correlations between VF_{INTRA}, TD_{EXTRA}, and gray matter concentration (GMC) in whole thalamus and its subregions. (A) Results for early-psychosis (EP) patients and their matched control group (n = 97). (B) Relationship patterns for the groups of patients with chronic schizophrenia (SCHZ) and their respective controls (n = 42). Significance: $P < .05$ (two-tailed) after False Discovery Rate (FDR) correction (q = 0.05).

correlations between VF_{INTRA} and TD_{EXTRA} (except for PuM-CL in HC_{EP}), confirming that these diffusion-derived parameters are largely dependent on each other (figure 3). By contrast, we found hardly no partial correlations between diffusion-derived parameters and GMC in HC_{EP}, HC_{SCHZ} and SCHZ (except for pulvinar in HC_{EP} and SCHZ, and PuM-CL in HC_{EP}). SCHZ and HC_{SCHZ} displayed overall similar partial correlations (except for a VF_{INTRA}/GMC correlation in pulvinar of SCHZ, and a trend for a weaker relationship between VF_{INTRA} and TD_{EXTRA} in many subregions of SCHZ, figure 3B, table 2). In contrast to the other groups, EP presented partial negative correlations between GMC and diffusion-derived parameters (either VF_{INTRA} or TD_{EXTRA}) within all subregions, except LP-VP and VP-VL (figure 3A). Thus, the relationship between

Downloaded from https://academic.oup.com/schizophreniabulletin/article/49/1/196/6692485 by EPF Lausanne (Inactive) user on 29 March 2023

Table 2. Summary of Alterations in EP and SCHZ Relative to Age-, Sex-Matched Healthy Controls (HC_{EP} and HC_{SCHZ})

	Healthy Controls vs Early Psychosis							
	Group Differences HC_{EP} vs EP[a,b]					Differences in Partial Correlations[c]		
	VF_{INTRA}	MD_{EXTRA}	TD_{EXTRA}	$DIFF_{INTRA}$	GMc	VF_{INTRA}/ TD_{EXTRA}	VF_{INTRA}/ GMC	TD_{EXTRA}/ GMC
Whole thalamus	↓		↑				$r_{HC} < r_{EP}$	
Pulvinar	↓		↑		↓	$r_{HC} < r_{EP}$	$r_{HC} < r_{EP}$	$r_{HC} < r_{EP}$
Ventral anterior	↓	↑	↑			$r_{HC} < r_{EP}$	$r_{HC} < r_{EP}$	
Mediodorsal	↓		↑		↓		$r_{HC} < r_{EP}$	
Lateral posterior-ventral posterior group	↓	↑	↑		↓			
Pulvinar medial-centrolateral group	↓			↓		$r_{HC} < r_{EP}$		$r_{HC} < r_{EP}$
Ventrolateral	↓							$r_{HC} < r_{EP}$
Ventral posterior-ventrolateral group.	↓		↑					
	Healthy Controls vs Schizophrenia							
	Group Differences HC_{SCHZ} vs SCHZ[a,b,c]					Differences in Partial Correlations		
	VF_{INTRA}	MD_{EXTRA}	TD_{EXTRA}	$DIFF_{INTRA}$	GMc	VF_{INTRA}/ TD_{EXTRA}	VF_{INTRA}/ GMC	TD_{EXTRA}/ GMC
Whole thalamus						$r_{HC} > r_{SCHZ}$	$r_{HC} > r_{SCHZ}$	
Pulvinar						$r_{HC} > r_{SCHZ}$	$r_{HC} < r_{SCHZ}$	
Ventral anterior		↑				$r_{HC} > r_{SCHZ}$		
Mediodorsal					↓	$r_{HC} > r_{SCHZ}$		
Lateral posterior-ventral posterior group					↓			
Pulvinar medial-centrolateral group					↓			
Ventrolateral						$r_{HC} > r_{SCHZ}$		
Ventral posterior-ventrolateral group								

Note: GMC, Gray matter concentration.
[a]Significant differences after False Discovery Rate (FDR) correction ($q = 0.05$) are presented.
[b]Healthy controls > Patients (↓) and Healthy controls < Patients (↑).
[c]The differences between groups in absolute correlation values (r) that are bigger than 0.1 are presented.

diffusion-derived parameters and GMC diverged most remarkably between EP and HC_{EP}. Moreover, the changes in the relationship between VF_{INTRA}, TD_{EXTRA}, and GMC in EP as compared to HC_{EP} differed across subregions (figure 3A, see pulvinar versus PuM-CL versus mediodorsal).

In summary, the association patterns between metrics in EP are stronger compared to other groups, further suggesting that the nature of the alterations occurring during the first years of psychosis is dominant and varies between subregions (see figure 3 and table 2).

Correlations With Clinical Data

We finally checked for associations between SMT-derived metrics and clinical symptoms, global functioning, and illness duration. After correction for multiple comparisons, the following correlations survived. In EP but not SCHZ, duration of illness correlated negatively with GMC in the whole thalamus, pulvinar, MD, LP-VP, VL, and VP-VL (table ST17), suggesting a rapid GMC decrease during the first years of illness. In SCHZ, negative symptoms correlated with diffusion-derived parameters (MD_{EXTRA}, TD_{EXTRA}, $DIFF_{INTRA}$) in PuM-CL (table ST18), while GAF scores correlated with GMC in whole thalamus, MD, PuM-CL, LP-VP, and pulvinar (table ST19) and with $DIFF_{INTRA}$ in all subregions (table ST20).

Discussion

To the best of our knowledge, this is the first study performing a multimodal assessment of thalamus integrity at the level of subregions in patients at the early and chronic stages of psychosis. This approach revealed that alterations of diffusion-related parameters and decreased GMC are already present in the early phase of psychosis and do not further worsen during the chronic stage. While our results confirm published data that the mediodorsal, posterior, and anterior regions are affected, our multimodal approach strongly suggests that the nature of the alterations varies across subregions.

Downloaded from https://academic.oup.com/schizophreniabulletin/article/49/1/196/6692485 by EPF Lausanne (Inactive) user on 29 March 2023

We also discovered previously unreported widespread diffusion-related alterations across the whole thalamus in EP when compared with age-matched HCs. Finally, the observed correlations between global functioning and microstructural parameters within many thalamic subregions (mostly in mediodorsal and posterior subregions) in SCHZ highlight the potent contribution of thalamus-related anomalies to a wide range of dysfunction and symptoms impacting everyday life.

Although our study is cross-sectional, the prominent abnormalities of microstructural organization in the thalamus of EP compared to HC_{EP} point towards aberrant changes occurring during the first years of psychosis or even before the transition to psychosis. While SCHZ tends to have lower GMC than EP, GMC decreases with the duration of illness in EP but not in SCHZ despite a much wider range of illness duration. These suggest that GMC undergoes a rapid decrease around the emergence and first years of psychosis. By contrast, the diffusion-related metrics that differ in EP as compared to HC_{EP} do not change with the duration of illness, suggesting that the underlying diffusion-related anomalies are present before the emergence of psychosis and may relate in part to a genetic vulnerability. Indeed, reduced neurite density assessed by diffusion imaging in thalamus has been associated with high polygenic risk scores for schizophrenia.[49] The lack of difference in VF_{INTRA} and TD_{EXTRA} between SCHZ and HC_{SCHZ} is due to the fact that these diffusion-derived metrics tend to differ between HC_{EP} and HC_{SCHZ} but not between EP and SCHZ. VF_{INTRA} and TD_{EXTRA} may capture microstructural properties of the fiber tracts entering and/or projecting out of the thalamus as each of these metrics strongly correlates in the thalamus and WM. The difference in VF_{INTRA} and TD_{EXTRA} values between HC_{EP} (mean age: 24.9 years) and HC_{SCHZ} (mean age: 36.7 years) may thus relate to the dynamic quadratic changes in WM properties that occur in healthy subjects during the maturation (with a peak arising around the age of 30 years for most WM tracts[50]) and throughout the adult lifespan. Therefore, our data suggest abnormal dynamic changes in properties/organization of fibers and/or neurites within the thalamus of psychotic patients that are linked to anomalies occurring during the maturation period. This is in line with the widespread WM abnormalities affecting thalamo-cortical tracts.[51–53]

By contrast, GMC decrease and MD_{EXTRA} increase are restricted respectively to the mediodorsal, posterior thalamus, and the VA. This corroborates previous findings that these subregions encompassing high-order nuclei display the most consistent abnormalities in terms of volume, shape, GMC, and diffusion-derived features.[11,20,23,24,26,27,30,54] Alterations in high-order nuclei may be linked to specific developmental characteristics accounting for their vulnerability. First, neurons from sensory and nonsensory thalamic nuclei derive from distinct populations of progenitor cells,[55] which display different developmental features. Second, loss of excessive neurons and synaptic pruning in the thalamus generally occur during postnatal development,[56,57] with connectivity remodeling within the mediodorsal and pulvinar nuclei during a period extending into early adulthood. Thus, the mediodorsal nuclei, which form reciprocal connections with the prefrontal cortex, contribute to the late maturation of prefrontal cortical circuits and may in turn undergo a prolonged period of synaptic refinement during early adulthood. The pulvinar is also subjected to remodeling of its connectivity with the cortex where some pulvinar nuclei are switching from primary sensory during early life to high-order nuclei in adulthood.[58] Our multimodal study also revealed the novel finding that the nature of local anomalies varies from one subregion to another. Thus, we found a $DIFF_{INTRA}$ decrease in PuM-CL, but a GMC decrease in MD, LP-VP, and pulvinar in EP. Furthermore, changes in relationships between GMC and diffusion-derived metrics in EP as compared to HCs differ across subregions. This suggests that each subregion may undergo distinct patterns of microstructural alterations. The underlying histological and microstructural anomalies captured by diffusion-derived parameters and GMC remain however elusive. Postmortem studies report decreased neuronal and glial cell density,[2,18] altered membrane phospholipid contents and oligodendrocyte metabolism in the thalamus of schizophrenia patients,[59–61] inferring abnormal myelination, astrocytic function, energy metabolism, and cytoskeleton assembly. MRI-derived variables can be influenced positively and negatively by these types of alterations but also by the volume and composition of the extracellular space. Therefore, changes in diffusion-derived metrics and/or GMC cannot unequivocally be attributed to well-identified alterations of the tissue organization.

Finally, we found only a few relationships between MRI-derived variables in the thalamus and clinical data. In SCHZ, GAF correlates positively with GMC in mediodorsal, and posterior subregions and with $DIFF_{INTRA}$ in all subregions. This supports that altered microstructural organization across many thalamic subregions have a broad functional impact in psychotic patients. At last in SCHZ, negative symptoms correlate negatively with every diffusion-derived parameters in PuM-CL which is mostly composed of the medial pulvinar. This nucleus is connected to prefrontal regions, insula, posterior cingulate, parietal, and temporal cortices[62] whose activities were reported to be negatively correlated with negative symptoms.[63] Moreover, some negative dimensions have been associated with emotional processing abnormalities dependent on the amygdala[64] which receives afferents from the medial pulvinar. Thus, this subregion could play an instrumental role in the expression of negative symptoms. Contrary to SCHZ, GAF, and negative symptoms did not correlate with MRI-derived metrics in the thalamus of EP. The reasons

Downloaded from https://academic.oup.com/schizophreniabulletin/article/49/1/196/6692485 by EPF Lausanne (Inactive) user on 29 March 2023

are unclear but may relate to the fast dynamic changes of thalamic microstructural organization around the first years of psychosis and to more fluctuating symptoms and global functioning in EP as compared to stable SCHZ. Moreover, the relationship between subtle microstructure alterations in one brain region and clinical symptoms are complex because the symptoms may arise from functional alterations within many large-scale brain networks and are accompanied with compensatory mechanisms.

To conclude, our multimodal MRI study reveals both widespread alterations in thalamus, and local, heterogeneous anomalies particularly in the mediodorsal and posterior parts. The study also suggests that thalamic abnormalities may emerge around the time of transition to psychosis and worsen during the very first years of psychosis without further significant degradation during the chronic stage of schizophrenia. Thus, the development of these thalamic alterations may relate to the abnormal functional thalamocortical connectivity which progresses during the prodromal stage with worsening of functional outcome and emergence of first psychotic episodes.[5] Future longitudinal studies in high-risk subjects will determine whether some of the described anomalies are present before the development of psychosis and could represent neurobiological vulnerabilities and potential early imaging markers.

Supplementary Material

Supplementary material is available at https://academic.oup.com/schizophreniabulletin/.

Acknowledgments

This work was supported by the National Center of Competence in Research "SYNAPSY – "The Synaptic Bases of Mental Diseases" from the Swiss National Science Foundation (n°51AU40_125759), an interdisciplinary fund of the Faculty of Biology and Medicine of the Lausanne University, the Alamaya Foundation and Adrian & Simone Frutiger Foundation. We acknowledge access to the facilities and expertise of the CIBM Center for Biomedical Imaging, a Swiss research center of xcellence founded and supported by Lausanne University Hospital, University of Lausanne, Ecole polytechnique fédérale de Lausanne, University of Geneva and Geneva University Hospital. The authors have declared that there are no conflicts of interest in relation to the subject of this study.

References

1. Andreasen NC. The role of the thalamus in schizophrenia. *Can J Psychiatry. Revue canadienne de psychiatrie.* 1997;42:27–33. doi: 10.1177/070674379704200104.
2. Byne W, Hazlett EA, Buchsbaum MS, Kemether E. The thalamus and schizophrenia: current status of research. *Acta Neuropathol.* 2009;117:347–368. doi: 10.1007/s00401-008-0404-0.
3. Clinton SM, Meador-Woodruff JH. Thalamic dysfunction in schizophrenia: neurochemical, neuropathological, and in vivo imaging abnormalities. *Schizophr Res.* 2004;69:237–253.
4. McCarley RW, Wible CG, Frumin M, *et al*. MRI anatomy of schizophrenia. *Biol Psychiatry.* 1999;45:1099–1119.
5. Steullet P. Thalamus-related anomalies as candidate mechanism-based biomarkers for psychosis. *Schizophr Res.* 2020;226:147–157. doi: 10.1016/j.schres.2019.05.027.
6. Anticevic A, Haut K, Murray JD, *et al*. Association of thalamic dysconnectivity and conversion to psychosis in youth and young adults at elevated clinical risk. *JAMA Psychiatry.* 2015;72:882–891. doi: 10.1001/jamapsychiatry.2015.0566.
7. Antonucci LA, Taurisano P, Fazio L, *et al*. Association of familial risk for schizophrenia with thalamic and medial prefrontal functional connectivity during attentional control. *Schizophr Res.* 2016;173:23–29. doi: 10.1016/j.schres.2016.03.014.
8. Bernard JA, Orr JM, Mittal VA. Cerebello-thalamo-cortical networks predict positive symptom progression in individuals at ultra-high risk for psychosis. *Neuroimage Clin.* 2017;14:622–628. doi: 10.1016/j.nicl.2017.03.001.
9. Cao H, Chen OY, Chung Y, *et al*. Cerebello-thalamo-cortical hyperconnectivity as a state-independent functional neural signature for psychosis prediction and characterization. *Nat Commun.* 2018;9:3836. doi:10.1038/s41467-018-06350-7.
10. Cho KI, Shenton ME, Kubicki M, *et al*. Altered thalamocortical white matter connectivity: probabilistic tractography study in clinical-high risk for psychosis and first-episode psychosis. *Schizophr Bull.* 2016;42:723–731. doi:10.1093/schbul/sbv169.
11. Cho, KIK, Kwak YB, Hwang WJ, *et al*. Microstructural changes in higher-order nuclei of the thalamus in patients with first-episode psychosis. *Biol Psychiatry.* 2019;85:70–78. doi: 10.1016/j.biopsych.2018.05.019.
12. Cooper D, Barker V, Radua J, Fusar-Poli P, Lawrie SM. Multimodal voxel-based meta-analysis of structural and functional magnetic resonance imaging studies in those at elevated genetic risk of developing schizophrenia. *Psychiatry Res.* 2014;221:69–77. doi:10.1016/j.pscychresns.2013.07.008.
13. Harrisberger F, Buechler R, Smieskova R, *et al*. Alterations in the hippocampus and thalamus in individuals at high risk for psychosis. *NPJ Schizophr.* 2016;2:16033. doi:10.1038/npjschz.2016.33.
14. Huang AS, Rogers BP, Woodward ND. Disrupted modulation of thalamus activation and thalamocortical connectivity during dual task performance in schizophrenia. *Schizophr Res.* 2019;210:270–277. doi:10.1016/j.schres.2018.12.022.
15. Lawrie SM, Whalley H, Kestelman JN, *et al*. Magnetic resonance imaging of brain in people at high risk of developing schizophrenia. *Lancet (London, England)*. 1999;353:30–33. doi:10.1016/s0140-6736(98)06244-8.
16. Lawrie SM, Whalley HC, Abukmeil SS, *et al*. Brain structure, genetic liability, and psychotic symptoms in subjects at high risk of developing schizophrenia. *Biol Psychiatry.* 2001;49:811–823.
17. Lunsford-Avery JR, Orr JM, Gupta T, *et al*. Sleep dysfunction and thalamic abnormalities in adolescents at ultra high-risk for psychosis. *Schizophr Res.* 2013;151:148–153. doi:10.1016/j.schres.2013.09.015.

Downloaded from https://academic.oup.com/schizophreniabulletin/article/49/1/196/6692485 by EPF Lausanne (Inactive) user on 29 March 2023

18. Dorph-Petersen KA, Lewis DA. Postmortem structural studies of the thalamus in schizophrenia. *Schizophr Res.* 2017;180:28–35. doi:10.1016/j.schres.2016.08.007.
19. Steullet P, Cabungcal JH, Bukhari SA, *et al*. The thalamic reticular nucleus in schizophrenia and bipolar disorder: role of parvalbumin-expressing neuron networks and oxidative stress. *Mol Psychiatry.* 2018;23:2057–2065. doi:10.1038/mp.2017.230.
20. Coscia DM, Narr KL, Robinson DG, *et al*. Volumetric and shape analysis of the thalamus in first-episode schizophrenia. *Hum Brain Mapp.* 2009;30:1236–1245. doi:10.1002/hbm.20595.
21. Danivas V, Kalmady SV, Venkatasubramanian G, Gangadhar BN. Thalamic shape abnormalities in antipsychotic naive schizophrenia. *Indian J Psychol Med.* 2013;35:34–38. doi:10.4103/0253-7176.112198.
22. Harms MP, Wang L, Mamah D, *et al*. Thalamic shape abnormalities in individuals with schizophrenia and their nonpsychotic siblings. *J Neurosci.* 2007;27:13835–13842. doi:10.1523/jneurosci.2571-07.2007.
23. Janssen J, Alemán-Gómez Y, Reig S, *et al*. Regional specificity of thalamic volume deficits in male adolescents with early-onset psychosis. *Br J Psychiatry.* 2012;200:30–36. doi:10.1192/bjp.bp.111.093732.
24. Qiu A, Zhong J, Graham S, Chia MY, Sim K. Combined analyses of thalamic volume, shape and white matter integrity in first-episode schizophrenia. *NeuroImage.* 2009;47:1163–1171. doi:10.1016/j.neuroimage.2009.04.027.
25. Skatun KC, Kaufmann T, Brandt CL, *et al*. Thalamo-cortical functional connectivity in schizophrenia and bipolar disorder. *Brain Imaging Behav.* 2018;12:640–652. doi:10.1007/s11682-017-9714-y.
26. Pergola G, Selvaggi P, Trizio S, Bertolino A, Blasi G. The role of the thalamus in schizophrenia from a neuroimaging perspective. *Neurosci Biobehav Rev.* 2015;54:57–75. doi:10.1016/j.neubiorev.2015.01.013.
27. Aleman-Gomez Y, Najdenovska E, Roine T, *et al*. Partial-volume modeling reveals reduced gray matter in specific thalamic nuclei early in the time course of psychosis and chronic schizophrenia. *Hum Brain Mapp.* 2020;41:4041–4061. doi:10.1002/hbm.25108.
28. Huang AS, Rogers BP, Sheffield JM, *et al*. Thalamic nuclei volumes in psychotic disorders and in youths with psychosis spectrum symptoms. *Am J Psychiatry.* 2020;177:1159. doi:10.1176/appi.ajp.2020.19101099.
29. Rose SE, Chalk JB, Janke AL, *et al*. Evidence of altered prefrontal-thalamic circuitry in schizophrenia: an optimized diffusion MRI study. *NeuroImage.* 2006;32:16–22. doi:10.1016/j.neuroimage.2006.03.003.
30. Kemether EM, Buchsbaum MS, Byne W, *et al*. Magnetic resonance imaging of mediodorsal, pulvinar, and centromedian nuclei of the thalamus in patients with schizophrenia. *Arch Gen Psychiatry.* 2003;60:983–991. doi:10.1001/archpsyc.60.9.983.
31. Kaden E, Kelm ND, Carson RP, Does MD, Alexander DC. Multi-compartment microscopic diffusion imaging. *NeuroImage.* 2016;139:346–359. doi:10.1016/j.neuroimage.2016.06.002.
32. Zhang H, Schneider T, Wheeler-Kingshott CA, Alexander DC. NODDI: practical in vivo neurite orientation dispersion and density imaging of the human brain. *NeuroImage.* 2012;61:1000–1016. doi:10.1016/j.neuroimage.2012.03.072.
33. Roche A, Forbes F. In: Springer International Publishing, ed. *Medical Imaging and Computing Asisted Intervention (MICCAI)*. Boston, MA, USA: Springer International Publishing. 2014:771–778.
34. Birchwood M, Fiorillo A. The critical period for early intervention. *Psychiatr Rehabil Ski.* 2000;4:182–198.
35. Baumann PS, Crespi S, Marion-Veyron R, *et al*. Treatment and early intervention in psychosis program (TIPP-Lausanne): implementation of an early intervention programme for psychosis in Switzerland. *Early Interv Psychiatry.* 2013;7:322–328. doi:10.1111/eip.12037.
36. Andreasen NC, Pressler M, Nopoulos P, Miller D, Ho BC. Antipsychotic dose equivalents and dose-years: a standardized method for comparing exposure to different drugs. *Biol Psychiatry.* 2010;67:255–262. doi:10.1016/j.biopsych.2009.08.040.
37. Preisig M, Fenton BT, Matthey ML, Berney A, Ferrero F. Diagnostic interview for genetic studies (DIGS): inter-rater and test-retest reliability of the French version. *Eur Arch Psychiatry Clin Neurosci.* 1999;249:174–179. doi:10.1007/s004060050084.
38. Kay SR, Fiszbein A, Opler LA. The positive and negative syndrome scale (PANSS) for schizophrenia. *Schizophr Bull.* 1987;13:261–276.
39. Association, A. P. *Diagnostic and Statistical Manual of Mental Disorders*. 4th, text rev edn. The Australian and New Zealand journal of psychiatry, 2000.
40. Yung AR, Yuen HP, McGorry PD, *et al*. Mapping the onset of psychosis: the Comprehensive Assessment of At-Risk Mental States. *Aust N Z J Psychiatry.* 2005;39:964–971. doi:10.1080/j.1440-1614.2005.01714.x.
41. Esteban O, Birman D, Schaer M, *et al*. MRIQC: advancing the automatic prediction of image quality in MRI from unseen sites. *PLoS One.* 2017;12:e0184661. doi:10.1371/journal.pone.0184661.
42. Bastiani M, Cottaar M, Fitzgibbon SP, *et al*. Automated quality control for within and between studies diffusion MRI data using a non-parametric framework for movement and distortion correction. *NeuroImage.* 2019;184:801–812. doi:10.1016/j.neuroimage.2018.09.073.
43. Tournier JD, Smith R, Raffelt D, *et al*. MRtrix3: a fast, flexible and open software framework for medical image processing and visualisation. *NeuroImage.* 2019;202:116137. doi:10.1016/j.neuroimage.2019.116137.
44. Jenkinson M, Beckmann CF, Behrens TE, Woolrich MW, Smith SM. Fsl. *NeuroImage.* 2012;62:782–790. doi:10.1016/j.neuroimage.2011.09.015.
45. Avants BB, Tustison NJ, Stauffer M, *et al*. The Insight ToolKit image registration framework. *Front Neuroinf.* 2014;8:44. doi:10.3389/fninf.2014.00044.
46. Choi HS, Haynor DR, Kim Y. Partial volume tissue classification of multichannel magnetic resonance images-a mixel model. *IEEE Trans Med Imaging.* 1991;10:395–407. doi:10.1109/42.97590.
47. Fischl B, Salat DH, Busa E, *et al*. Whole brain segmentation: automated labeling of neuroanatomical structures in the human brain. *Neuron.* 2002;33:341–355.
48. Fortin JP, Parker D, Tunc B, *et al*. Harmonization of multi-site diffusion tensor imaging data. *NeuroImage.* 2017;161:149–170. doi:10.1016/j.neuroimage.2017.08.047.
49. Stauffer EM, Bethlehem RAI, Warrier V, *et al*. Grey and white matter microstructure is associated with polygenic risk for schizophrenia. *Mol Psychiatry.* 2021;26:7709–7718. doi:10.1038/s41380-021-01260-5.
50. Lebel C, Gee M, Camicioli R, *et al*. Diffusion tensor imaging of white matter tract evolution over the lifespan. *NeuroImage.* 2012;60:340–352. doi:10.1016/j.neuroimage.2011.11.094.

Downloaded from https://academic.oup.com/schizophreniabulletin/article/49/1/196/6692485 by EPF Lausanne (Inactive) user on 29 March 2023

51. Hamoda HM, Makhlouf AT, Fitzsimmons J, *et al*. Abnormalities in thalamo-cortical connections in patients with first-episode schizophrenia: a two-tensor tractography study. *Brain Imaging Behav.* 2019;13:472–481. doi:10.1007/s11682-018-9862-8.
52. Kelly S, Jahanshad N, Zalesky A, *et al*. Widespread white matter microstructural differences in schizophrenia across 4322 individuals: results from the ENIGMA Schizophrenia DTI Working Group. *Mol Psychiatry.* 2018;23:1261–1269. doi:10.1038/mp.2017.170.
53. Kim DJ, Kim JJ, Park JY, *et al*. Quantification of thalamocortical tracts in schizophrenia on probabilistic maps. *Neuroreport.* 2008;19:399–403. doi:10.1097/WNR.0b013e3282f56634.
54. Danos P, Baumann B, Kramer A, *et al*. Volumes of association thalamic nuclei in schizophrenia: a postmortem study. *Schizophr Res.* 2003;60:141–155.
55. Nakagawa Y. Development of the thalamus: from early patterning to regulation of cortical functions. Wiley interdisciplinary reviews. *Dev Biol.* 2019;8:e345. doi:10.1002/wdev.345.
56. Ferguson BR, Gao WJ. Development of thalamocortical connections between the mediodorsal thalamus and the prefrontal cortex and its implication in cognition. *Front Hum Neurosci.* 2014;8:1027. doi:10.3389/fnhum.2014.01027.
57. Schafer DP, Lehrman EK, Kautzman AG, *et al*. Microglia sculpt postnatal neural circuits in an activity and complement-dependent manner. *Neuron.* 2012;74:691–705. doi:10.1016/j.neuron.2012.03.026.
58. Homman-Ludiye J, Bourne JA. The medial pulvinar: function, origin and association with neurodevelopmental disorders. *J Anat.* 2019;235:507–520. doi:10.1111/joa.12932.
59. Martins-de-Souza D, Maccarrone G, Wobrock T, *et al*. Proteome analysis of the thalamus and cerebrospinal fluid reveals glycolysis dysfunction and potential biomarkers candidates for schizophrenia. *J Psychiatr Res.* 2010;44:1176–1189. doi:10.1016/j.jpsychires.2010.04.014 .
60. McCullumsmith RE, O'Donovan SM, Drummond JB, *et al*. Cell-specific abnormalities of glutamate transporters in schizophrenia: sick astrocytes and compensating relay neurons? *Mol Psychiatry.* 2016;21:823–830. doi:10.1038/mp.2015.148.
61. Schmitt A, Wilczek K, Blennow K, *et al*. Altered thalamic membrane phospholipids in schizophrenia: a postmortem study. *Biol Psychiatry.* 2004;56:41–45. doi:10.1016/j.biopsych.2004.03.019.
62. Benarroch EE. Pulvinar: associative role in cortical function and clinical correlations. *Neurology.* 2015;84:738–747. doi:10.1212/WNL.0000000000001276.
63. Shaffer JJ, Peterson MJ, McMahon MA, *et al*. Neural correlates of schizophrenia negative symptoms: distinct subtypes impact dissociable brain circuits. *Mol Neuropsychiatry.* 2015;1:191–200. doi:10.1159/000440979.
64. Millan MJ, Fone K, Steckler T, Horan WP. Negative symptoms of schizophrenia: clinical characteristics, pathophysiological substrates, experimental models and prospects for improved treatment. *Eur Neuropsychopharmacol.* 2014;24:645–692. doi:10.1016/j.euroneuro.2014.03.008.

Downloaded from https://academic.oup.com/schizophreniabulletin/article/49/1/196/6692485 by EPF Lausanne (Inactive) user on 29 March 2023